

ADVANCES IN TIME-RESOLVED MEASUREMENT OF MAGNETIC FIELD AND ELECTRON TEMPERATURE IN LOW-MAGNETIC-FIELD PLASMAS

D. J. Den Hartog,^{1,2} J. R. Ambuel,¹ M. T. Borchardt,¹ K. J. Caspary,¹ E. A. Den Hartog,¹ A. F. Falkowski,¹ W. S. Harris,¹ J. Ko,¹ N. A. Pablant,³ J. A. Reusch,¹ P. E. Robl,¹ H. D. Stephens,¹ H. P. Summers,⁴ and Y. M. Yang¹

¹University of Wisconsin–Madison, Madison, WI 53706 USA

²Center for Magnetic Self-Organization in Laboratory and Astrophysical Plasmas

³University of California–San Diego, La Jolla, CA 92093 USA

⁴University of Strathclyde, Glasgow G4 0NG, UK

e-mail of presenting author: djenhar@wisc.edu

Internal time-resolved measurement of magnetic field and electron temperature in low-field (≤ 1 T) plasmas is a difficult diagnostic challenge. To meet this diagnostic challenge in the Madison Symmetric Torus reversed-field pinch, two techniques are being developed: 1) spectral motional Stark effect (MSE) and 2) Fast Thomson scattering. For spectral MSE, the entire Stark-split H α spectrum emitted by hydrogen neutral beam atoms is recorded and analyzed using a newly refined atomic emission model. A new analysis scheme has been developed to infer both the polarization direction and the magnitude of Stark splitting, from which both the direction and magnitude of the local magnetic field can be derived. For Fast Thomson scattering, two standard commercial flashlamp-pumped Nd:YAG lasers have been upgraded to “pulse-burst” capability. Each laser produces a burst of up to fifteen pulses at repetition rates 1–12.5 kHz, thus enabling recording of the dynamic evolution of the electron temperature profile and electron temperature fluctuations. To further these capabilities, a custom pulse-burst laser system is now being commissioned. This new laser is designed to produce a burst of laser pulses at repetition frequencies 5 – 250 kHz.

I. INTRODUCTION

Several types of fusion research devices such as magnetic mirrors, small-aspect-ratio tori, and reversed-field pinches are characterized by relatively low internal magnetic field (≤ 1 T) over some or all of the plasma volume. Internal time-resolved measurement of magnetic field and electron temperature in such low-field plasmas is a difficult diagnostic challenge. Techniques employed in the higher-field plasmas of tokamaks and stellarators are often not applicable. For example, the polarimetry-

based motional Stark effect (MSE) measurement of magnetic field is very difficult to implement at low field because the components of the Stark spectrum are not sufficiently separated.¹ Electron cyclotron emission (ECE) measurement of electron temperature often does not work at low field because the plasma is typically overdense ($\omega_{pe} > \omega_{ce}$).² To meet these diagnostic challenges in the low-field plasma in the Madison Symmetric Torus (MST) reversed-field pinch (RFP), we are continuing development of two techniques: spectral MSE to measure internal magnetic field (Sec. II), and Fast Thomson scattering to measure electron temperature (Sec. III).

The RFP configuration can be characterized as toroidal magnetic confinement of high-temperature plasma with low applied magnetic field.³ The toroidal field in an RFP is typically ten times smaller than a tokamak of similar plasma current. The plasma equilibrium is determined largely by self-generated plasma currents, thus internal magnetic field and electron temperature measurements are critical to equilibrium reconstruction.⁴ In a typical MST plasma, the maximum magnetic field is 0.5 T, density is approximately 10^{19} m⁻³, electron and ion temperatures less than 2 keV, and plasma current less than 500 kA. The MST device has a major radius of 1.5 and a minor radius of 0.5 m.

II. SPECTRAL MSE

For spectral MSE, the entire Stark-split H α spectrum emitted by hydrogen neutral beam atoms injected into the plasma is recorded and analyzed to obtain a local measurement of magnetic field \mathbf{B} .^{5,6} Spectral MSE is an application of beam emission spectroscopy; the beam atoms with velocity \mathbf{v} are excited by collisions with plasma electrons and then radiate at characteristic emission lines. The neutral hydrogen beam atom energy

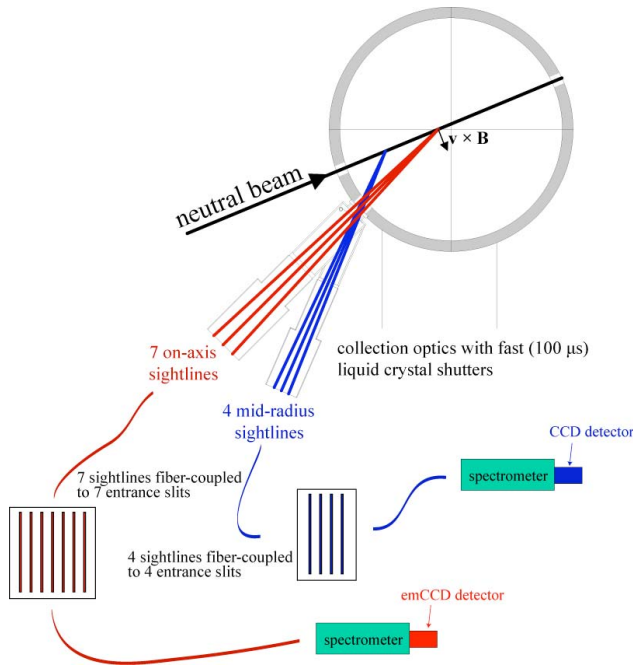


Fig. 1. The MSE diagnostic has an on-axis view and a new mid-radius view. Each view contains multiple sightlines of the diagnostic neutral beam.

levels are split by the motional electric field $\mathbf{E} = \mathbf{v} \times \mathbf{B}$. The resulting $H\alpha$ ($n = 3 \rightarrow 2$) spectrum contains nine components of various amplitudes and polarizations.⁷ Both the direction and magnitude of the local \mathbf{B} can be inferred from the polarization direction and wavelength splitting of the motional Stark spectrum (the velocity of the beam is accurately known and thus \mathbf{B} is the remaining unknown).⁸

Figure 1 is an illustration of the MSE diagnostic on MST, viewing a cross-section cut through the MST plasma. The on-axis view collects beam emission from the current axis of the plasma, which is shifted outward from the geometric center of the cross-section. The mid-radius view crosses the beam near the half-radius of the plasma column. The diagnostic neutral beam (DNB) is operated at a nominal energy of 46 kV with a maximum beam current of 5.5 A for a 20 ms pulse (roughly equivalent to the length of the equilibrium flat-top period of an MST discharge). At the on-axis measurement point, the magnetic field is toroidal (out of the page in Fig. 1) and hence only one direction (vertical) of polarization need be measured to accurately determine the magnetic field. The relative amounts of light in the π and σ lobes of the Stark emission pattern are completely determined by the geometry of the sight lines and the beam. At the mid-radius measurement point, the magnetic field is roughly equal parts toroidal and poloidal. The angle can change significantly from shot to shot and during a single shot. This forces simultaneous measurement of two orthogonal

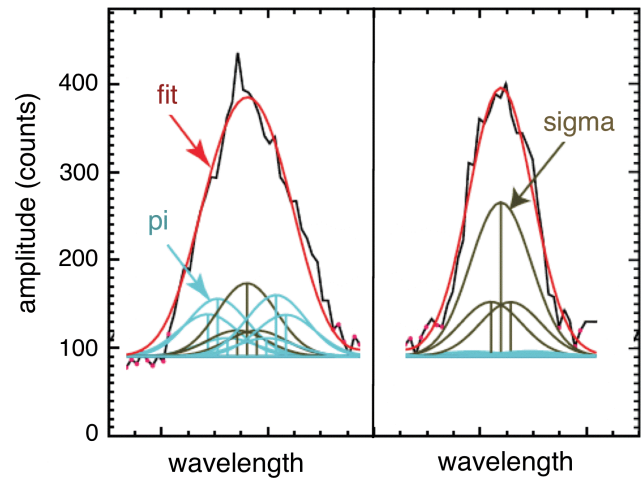


Fig. 2. Sample spectra from the mid-radius view, the two panels containing spectra from two sightlines set up to collect orthogonal polarizations simultaneously. The position and broadening of the π and σ components are illustrated, along with the fit to the recorded spectra. The derived $|\mathbf{B}| = 0.42 \pm 0.07$ T and the pitch angle $\gamma = 40.3^\circ \pm 9.4^\circ$.

polarizations in order to accurately determine the magnetic field strength.⁸ Measurement of the two polarizations also provides information on the magnetic field pitch angle although this is more prone to systematic errors. The situation is not as difficult as in the tokamak, however, since the precision needed on the field line angle in the RFP is not as great (the field direction changes by more than 90° between on-axis and edge). The optical elements in the mid-radius view provide four sightlines of the beam, grouped into two sets of two orthogonal polarizations. A sample Stark spectrum from the mid-radius view is shown in Fig. 2.

Beam emission collected by the sightlines in each of the views is transported via fiber optics to the entrance slit arrays of two spectrometers (Fig. 1). Light from the four or seven entrance slits is simultaneously recorded on a single frame of the detector mounted on the exit plane of each spectrometer. Spectral overlap is avoided because each of the sightlines is equipped with a narrow-band interference filter that passes only the Doppler-shifted $H\alpha$ beam emission.

Each of the sightlines is also equipped with a fast ferroelectric liquid crystal shutter (Displaytech, Inc.). The trigger and exposure times of each shutter are independently controlled, with minimum exposure time of 100 μ s. In practice, the shutters in each view are fired sequentially, resulting in a time sequence of Stark spectra on each detector frame (Fig. 3). This enables high-speed recording of MSE data, with effective data rates of 2-3 kHz using the emCCD (electron-multiplying CCD) detector on the spectrometer connected to the on-axis sightlines.

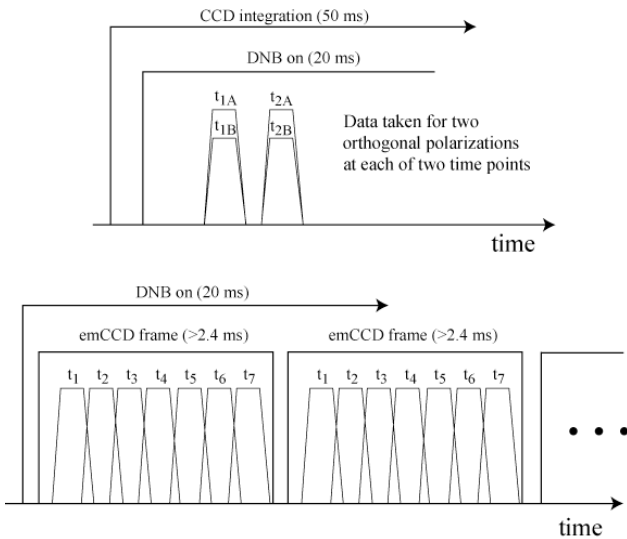


Fig. 3. Timing diagrams illustrating the sequence of events during operation of the MSE diagnostic. The lower diagram represents collection of seven sequential spectra from the on-axis view on a single emCCD frame, a sequence repeated after each frame is read out; multiple such sequences are recorded during each 20 ms DNB pulse. The upper diagram represents collection of two sequential sets of spectra from the mid-radius view on a single CCD frame, not repeated during a DNB pulse because the CCD frame readout is slow.

Improved modeling of the relative magnitudes and positions of the Stark multiplets is underway. This model includes spin-orbit coupling and Zeeman effects. At low \mathbf{B} field values (~ 0.1 T) the motional Stark splitting becomes comparable to the fine structure splitting due to spin-orbit coupling. Additionally, our previous modeling assumed that all beam atom energy levels were populated in proportion to their statistical weights and the relative brightness of each Stark manifold component was set accordingly. This assumption may be invalid if the beam energy levels have not been fully mixed by collisions along the beam path. In particular, for measurement points like the mid-radius view, the beam has travelled through only about 25 cm of plasma and may not be fully mixed. Therefore, we are exploring possible means of incorporating non-statistical weights into our spectral model.

III. FAST THOMSON SCATTERING

Figure 4 illustrates the layout of the Thomson scattering diagnostic system on MST.^{9,10} This system was designed to produce accurate profile measurements for $10 \text{ eV} < Te < 2 \text{ keV}$ at electron densities $\geq 10^{18} \text{ m}^{-3}$. Scattered light is simultaneously recorded from 21 radial locations across the 0.5 m minor radius of the plasma.

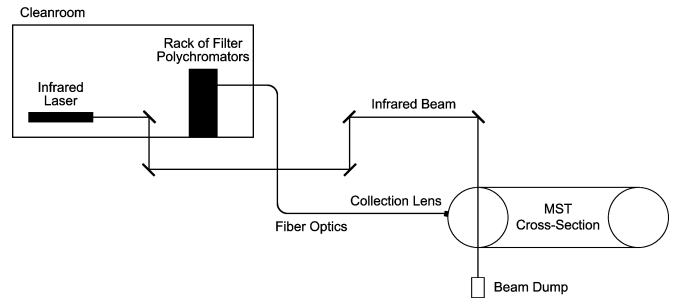


Fig. 4. Layout of the Thomson scattering diagnostic on MST. The laser systems and banks of filter polychromators are in a temperature-controlled room approximately 12 m remote from the MST torus.

Multi-pulse capability is provided by two standard commercial flashlamp-pumped Nd:YAG lasers that have been upgraded to pulse-burst capability. Each laser produces a burst of up to fifteen 2 J Q -switched pulses (1064 nm) at repetition rates 1–12.5 kHz.^{11,12} This enables collection of thirty Te profiles during a single MST discharge, at rates varying from 1–25 kHz. Scattered light is collected by a custom deep-focus lens and coupled by optical fiber to 21 identical filter polychromators.

The 25 kHz measurement rate of the upgraded Nd:YAG lasers is sufficient to measure the effect of a magnetic island on the profile as the island rapidly rotates by the measurement point. In other words, we are now able to measure the Te fluctuations associated with magnetic islands formed by tearing reconnection in the MST plasma.¹³ These islands have a significant impact on the thermal characteristics of magnetically confined plasmas such as the RFP. In standard plasmas with a spectrum of tearing modes, islands tend to flatten the Te profile across resonant surfaces, as observed in tokamaks. In striking contrast, a temperature gradient within an island is observed immediately following a sawtooth event when a single core tearing mode dominates. This suggests local heating and relatively good confinement within the island.

To further the capability to make fast Thomson scattering measurements on MST, we are constructing a “pulse-burst” laser system for addition to the Thomson scattering diagnostic.^{14,15} The goal is to record fast equilibrium changes in the electron pressure, and measurements of turbulence and electron pressure fluctuations.

The pulse-burst laser system is the only novel component being developed for this extension of the Thomson scattering diagnostic on MST. It is designed to produce a “burst” train of 1–2 J pulses, each pulse < 100 ns in duration. At lower pulse repetition frequencies (≤ 50 kHz), the burst train will be up to 20 ms long. At higher pulse repetition frequencies each burst train will be

constrained to 10-30 pulses, although it is likely that multiple such burst trains can be produced during a single MST discharge. The duty cycle for production of these burst trains is low (≤ 2 minutes), set by the duty cycle of MST and the thermal cooling time of the laser rods. The pulse-burst laser system will function as an adjunct to the existing commercial Nd:YAG lasers used for Thomson scattering on MST. It will use the same beamline and optics, and is being assembled in an adjoining room. The rest of the Thomson scattering hardware (polychromators, detectors, digitizers, etc.) is already capable of recording the burst trains described above.

This new laser system will operate at 1064 nm and is a master oscillator, power amplifier architecture. The master oscillator is a compact diode-pumped Nd:YVO₄ laser, intermediate amplifier stages are flashlamp-pumped Nd:YAG, and final stages will be flashlamp-pumped Nd:glass(silicate). Variable pulse-width drive (0.3-20 ms) of the flashlamps is accomplished by insulated gate bipolar transistor (IGBT) switching of large electrolytic capacitor banks.¹⁴ Flashlamp power supply commissioning is nearly complete, and the laser system itself is being assembled.

ACKNOWLEDGMENTS

Figures 1 and 3 are courtesy of Darren Craig. This work is supported by the United States Department of Energy and the National Science Foundation.

REFERENCES

1. M. KULDKEPP, M. J. WALSH, P. G. CAROLAN, N. J. CONWAY, N. C. HAWKES, J. MCCONE, E. RACHLEW, and G. WEARING, "Motional Stark effect diagnostic pilot experiment for MAST," *Rev. Sci. Instrum.* **77**, 10E905 (2006).
2. P. K. CHATTOPADHYAY, J. K. ANDERSON, T. M. BIEWER, D. CRAIG, C. B. FOREST, R. W. HARVEY, and A. P. SMIRNOV, "Electron Bernstein wave emission from an overdense reversed field pinch plasma," *Phys. Plasmas* **9**, 752 (2002).
3. H. A. B. BODIN and A. A. NEWTON, "Reversed-field-pinch research," *Nucl. Fusion* **20**, 1255 (1980).
4. J. K. ANDERSON, C. B. FOREST, T. M. BIEWER, J. S. SARFF, and J. C. WRIGHT, "Equilibrium reconstruction in the Madison Symmetric Torus reversed field pinch," *Nucl. Fusion* **44**, 162 (2004).
5. D. J. DEN HARTOG, D. CRAIG, D. A. ENNIS, G. FIKSEL, S. GANGADHARA, D. J. HOLLY, J. C. REARDON, V. I. DAVYDENKO, A. A. IVANOV, A. A. LIZUNOV, M. G. O'MULLANE, and H. P. SUMMERS, "Advances in neutral-beam-based diagnostics on the Madison Symmetric Torus reversed-field pinch," *Rev. Sci. Instrum.* **77**, 10F122 (2006).
6. N. A. PABLANT, K. H. BURRELL, R. J. GROEBNER, C. T. HOLCOMB, and D. H. KAPLAN, "Measurements of the internal magnetic field using the B-Stark motional Stark effect diagnostic on DIII-D," *Rev. Sci. Instrum.* **81**, 10D729 (2010).
7. H. R. GRIEM, *Principles of Plasma Spectroscopy*, p. 310, Cambridge University Press, Cambridge, UK (1997).
8. J. KO, D. J. DEN HARTOG, K. J. CASPARY, E. A. DEN HARTOG, N. A. PABLANT, and H. P. SUMMERS, "Two-point motional Stark effect diagnostic for Madison Symmetric Torus," *Rev. Sci. Instrum.* **81**, 10D702 (2010).
9. J. A. REUSCH, M. T. BORCHARDT, D. J. DEN HARTOG, A. FALKOWSKI, D. J. HOLLY, R. O'CONNELL, and H. D. STEPHENS, "Multi-point Thomson Scattering Diagnostic for the Madison Symmetric Torus Reversed-Field Pinch," *Rev. Sci. Instrum.* **79**, 10E733 (2008).
10. R. O'CONNELL, D. J. DEN HARTOG, J. A. REUSCH and H. D. STEPHENS, "Optimizing a Thomson scattering diagnostic for fast dynamics and high background," *Rev. Sci. Instrum.* **79**, 10E735 (2008).
11. D. J. DEN HARTOG, J. R. AMBUEL, M. T. BORCHARDT, J. A. REUSCH, P. E. ROBL, and Y. M. YANG, "Pulse-burst operation of standard Nd:YAG lasers," *J. Phys.: Conf. Ser.* **227**, 012023 (2010).
12. D. J. DEN HARTOG, J. R. AMBUEL, M. T. BORCHARDT, A. F. FALKOWSKI, W. S. HARRIS, D. J. HOLLY, E. PARKE, J. A. REUSCH, P. E. ROBL, H. D. STEPHENS, and Y. M. YANG, "Pulse-burst laser systems for fast Thomson scattering," *Rev. Sci. Instrum.* **81**, 10D513 (2010).
13. H. D. STEPHENS, D. J. DEN HARTOG, C. C. HEGNA, and J. A. REUSCH, "Electron thermal transport within magnetic islands in the reversed-field pinch," *Phys. Plasmas* **17**, 056115 (2010).
14. D. J. DEN HARTOG, N. JIANG, and W. R. LEMPERS, "A pulse-burst laser system for a high-repetition-rate Thomson scattering diagnostic," *Rev. Sci. Instrum.* **79**, 10E736 (2008).
15. W. S. HARRIS, D. J. DEN HARTOG, and N. C. HURST, "Initial operation of a pulse-burst laser system for high-repetition-rate Thomson scattering," *Rev. Sci. Instrum.* **81**, 10D505 (2010).